A Remote Sensing Approach for Identifying and Mapping the Coastal Urban Heat Island in Bangladesh through Temperature Modeling

M. R. Ashikur[1]*, M. H. Sazzad[2], R. S. Rupom[3]

Abstract

The coastal urban region is one of the economic hubs of development in Bangladesh and its land use/ land cover (LULC) and land surface temperature (LST) have been changing continuously for massive upliftment which gives the aftermath of the urban heat island (UHI). This study explored the pattern of LULC and LST changes for the years 2010, 2015, and 2020 and identified the hot and cool locations in 2020 of the Khulna Development Authority (KDA) area. Landsat 7 enhanced thematic mapper (ETM) multitemporal images were used and remote sensing (RS) and geographical information system (GIS) techniques were applied for identifying and mapping the output. The results have mentioned that almost 19 % of the buildup area has increased in 2020 compared to 2010 whereas it dominates the loss of wetland vegetation, water bodies, agricultural land, and trees and bushes. The contribution index (CI) has revealed that increasing buildup areas promote to raise in the LST which has increased around 7^{o} C over the past decade. The study also identified that about 28 Mouzas were considered hot islands in 2020. This study will be helpful to understand the impacts of LST change and potential hot and cool islands to propound appropriate policy measures to superintend it.

Keywords: Remote Sensing; Geographical Information System; Land Surface Temperature; Contribution index; Coastal Urban area.

1. Introduction

Many coastal urban areas have undergone a surge of rapid urbanization leading to severe environmental issues. Tremendous and speedy urbanization in the coastal urban areas has also caused increasingly serious impacts on the coastal ecosystem. With

[1] * *Institute of Bay of Bengal & Bangladesh Studies, Bangabandhu Sheikh Mujibur Rahman Maritime University, Dhaka, Bangladesh.*

[2] *Department of Urban & Regional Planning, Khulna University of Engineering & Technology, Khulna, Bangladesh.*

[3] *Department of Urban & Regional Planning, Rajshahi University of Engineering & Technology, Rajshahi, Bangladesh.*
*Corresponding Author's E-mail
ro.ibbbs@bsmrmu.edu.bd

sudden coastal urbanization, the urban elements face enormous problems like tremendous land use/land cover (LULC), ecological imbalance, and irregular land surface temperature (LST) that create urban heat islands (UHI).). The conversion of wetlands and other land surfaces into buildup areas is expedited by urbanization and root cause for LULC change, which is one of the key causes of increasing urban areas LST (Tran et al. 2017, 119-132; Halmy et al. 2015, 101-112; Mishra and Rai 2016, 249; Pal and Ziaul 2017, 125-145). The changes in LULC subsequently increase the LST to form UHI which has a direct linkage with high energy consumption, air pollution, and human health risks (Ahmed 2011, 43; Pal and Ziaul 2017, 125-145). The formation of UHI creates distinct thermal and climatic conditions in urban areas which affect the lives of the inhabitants and the overall environment of any coastal urban area (Jain et al. 2020, 54-66; Voogt and Oke 2003, 370-384).

A long-term consequence of LULC change is the increment of LST in urban areas (Maimaitiyiming et al. 2014, 59-66; Tan et al. 2009, 525-529). Therefore, monitoring LULC transformation and analysis of LST are very essential for better environmental management, sustainable climate change mitigation, and resilience strategies (Balew and Korme 2020). That is why the urban indices (UI) are considered for the parameters to identify the actual relationship between LULC and LST. Among them the soil-adjusted vegetation index (SAVI) defines the coverage of urban area (Ren, Zhou, and Zhang 2018, 439-445), enhance bareness and buildup index (EBBI) indicates the distribution of bare land (Mushore et al. 2017a, 397-410), normalized difference built-up index (NDBI) separates built-up areas (Balew and Korme 2020; Zha, Gao, and Ni 2003, 583-594), normalized difference water index (NDWI) is used to select water and vegetation liquid (Dasgupta et al. 2015, 205-242; Gao 1995, 225-236), normalized difference vegetation index (NDVI), which is based on vegetation ratio (Balew and Korme 2020). Heat waves in an urban area mainly occur due to the high concentration of atmospheric temperature (Jain et al. 2020, 54-66). In high surface temperature areas, the hot weather and heat waves have a considerable negative impact on the lives of the inhabitants (Tran et al. 2017, 119-132). The contribution index (CI) describes urban growth and its responses to LST in an urban area (Tarawally et al. 2018, 112).

Change detection in LULC scenarios and LST monitoring through direct field visits are time-consuming, labor-intensive, and error-prone (Lilly Rose and Devadas 2009). Besides, the integration of remote sensing (RS) and geographical information system (GIS) technologies is efficient to evaluate, monitoring, and model LULC and LST changes (Fu and Weng 2018, 123-135; Trolle et al. 2019, 627-633). GIS and RS approaches are found fruitful in several studies in estimating LULC, LST, and UHI phenomena over urban ecosystems (Balogun and Ishola 2017, 22-31; El-Zeiny and Effat 2017, 266-277; Perugini et al. 2017, 053002; Rasul 2020). Change detection is the process of determining and/or describing changes in LULC characteristics based on co-registered multi-temporal RS data (Elagouz et al. 2019) and RS spectral index is a good method to classify LULC classes (Chen et al. 2006, 133-146). The moderate resolution multispectral Landsat satellite products; i.e. thematic mapper (TM), enhanced thematic mapper (ETM+), and operational land imager (OLI)/ thermal infrared sensor (TIRS) data of advanced spaceborne thermal emission and reflection radiometer (ASTER) have been used for estimating spatiotemporal LST (Chun and Guldmann 2014, 76-88; Guo et al. 2015, 1-10; Wu et al. 2011, 1-8).

In recent years, several studies on different integrated modeling approaches have already been applied to identify the relationship between LULC and LST. Li et al. 2020 quantified the diurnal and seasonal surface UHI intensity in global 419 major cities during the period 2003-2013 by applying geographically weighted regression (GWR), ordinary least square (OLS), and multiple linear regression model (MLRM) (Li, Zha, and Zhang 2020, 102131). Rahman et al. 2017 used Landsat imageries and the Cellular Automata (CA) model to investigate the effects of LULC changes on LST for Saudi Arabia's eastern coastal city of Dammam (Rahman, Aldosary, and Mortoja 2017, 36). For, Bangladesh, Ahmed et al. 2013 first calculated decadal shifts of LULC and LST from Landsat sensors in the Dhaka metropolitan area (Ahmed et al. 2013, 5969-5998).

The present research has explored the change in LULC and LST patterns and also identified the hot and cool islands that were not flourished in coastal urban areas in Bangladesh. Such kinds of research are necessary for the coastal urban people as well as sustainable coastal urban development. The research finds out the hot and cool locations in the coastal urban area considering the LST where LULC and UI like NDWI, NDVI, NDBI, SAVI, and EBBI are responsible for the LST.

2. Materials and Methods

2.1 Research area

The research area is in Khulna district which is one of 19 coastal areas in Bangladesh. The research area has consisted of 81 Mouzas of Khulna development authority's (KDA) geographical territory and is situated between latitude 22o 12' to 23o 59' North and longitude 89o 14' to 89o 45' East covering an area of approximately 202.54 sqr km (Fig. 1). The study area is situated about 2.5 meters below sea level (Esraz-Ul-Zannat 2012). According to the Bangladesh population census 2011, the population density of the study area was about 1.61% of the total national population of Bangladesh. During April and May, the area experiences the highest temperature. Besides, the area perceives the minimum temperature between 8.8o C and 27o C and the maximum temperature to vary between 23.6o C to 34.4o C (BBS 2019). According to the Bangladesh Meteorological Department (BMD), in 2019 average annual rainfall was 1809 mm.

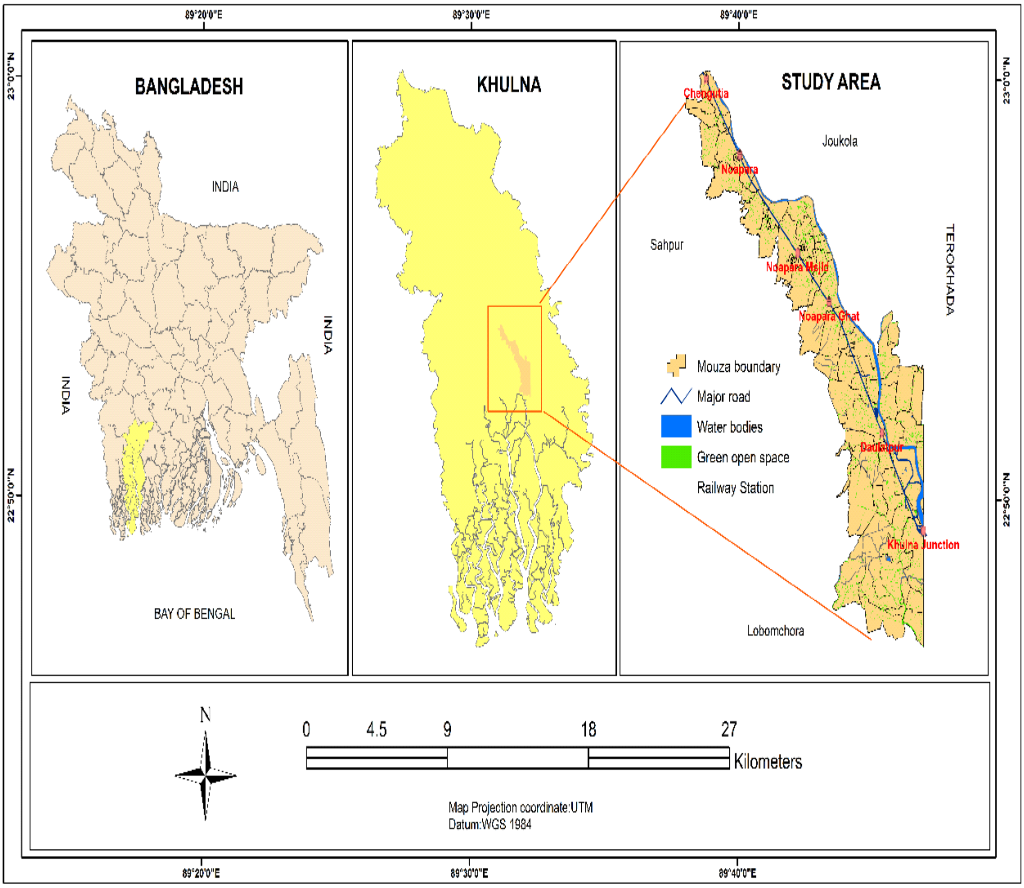

Figure 1: Study area map. The map represents 81 mouzas boundary along with the major roads, water bodies and green open spaces in the KDA area.

2.2 Data description and processing

In the present study, Landsat 7 enhanced thematic mapper (ETM) imaginary data were used, and these were collected from the United States Geological Survey (USGS) (https://earthexplorer.usgs.gov/) for the years 2010, 2015, and 2020. For calculating LST in the study area, all the Landsat data in the specific years were collected considering the dry or summer season (Mustafa et al. 2020). All the satellite images were downloaded with the set of maximum cloud cover of < 30% for cloud-free images. Information on the Landsat images (date, spatial resolution, sensor, cloud cover, and path/row) obtained from the USGS online data repository is summarized in Table 1.

Table 1: Information on Landsat satellite images

Satellite images	Data acquired	Sensor	Cloud cover	Spatial resolution	Path/Row
Landsat 7	16 April, 2010	ETM	< 30%	30m	135/43
Landsat 7	20 April, 2015	ETM	< 30%	30m	135/43
Landsat 7	08 April, 2020	ETM	< 30%	30m	135/43

To do the scan line correction (SLC) for the Landsat 7 data for each band, a scan gap mask was developed that identified existing data as 1 and missing data in the scan gap and filled regions as 0. The pixel values of the SLC-off image were met (the ‘primary scene’) and the pixel values of an SLC-on image (the 'fill scene') were constructed by adding corrective gain and bias. To fill the scene gap, equation (1) was applied to develop a linear histogram that resulted in a linear transformation between one image and another.

$Y \approx GX + B$ ……………………………..……... (1)

Here, G = the gain used to histogram match the fill image to the primary image.

B = the bias used to histogram match the fill image to the primary image.

X = the fill (SLC-on) scene array.

Y = the primary (SLC-off) scene array.

The corrective gain and bias were assessed by using the mean and standard deviation of the data.

$G = \frac{\sigma_Y}{\sigma_X}$ ………………………………………………………….......................... (2)

$B = \bar{Y} - G\bar{X}$ ………….................…………………………………………..(3)

Here, σ_X = the standard deviation of data in fill image X.

σ_Y = the standard deviation of data in primary image Y.

$\bar{X}$ = the mean of the fill (SLC-on) scene array.

$\bar{Y}$ = the mean of the primary (SLC-off) scene array.

2.3. Multitemporal Land Use/ Land Cover (LULC) Mapping

The acquired Landsat images were used to land cover classification for the years 2010, 2015, and 2020 based on the maximum likelihood supervised classification (MLSC) method. The obtained Landsat data were enhanced by using (3x3) majority filter techniques in Erdas Imagine software v.15 for better visibility. By selecting training samples for distinct LULC classes, a True Color Composite (TCC) was created for all of the images using appropriate band combinations (Chapa, Hariharan, and Hack 2019, 5266). The LULC area was categorized into five classes i.e., water bodies, trees and bushes, agricultural land, wetland vegetation, and buildup area based on MLSC (Table 2). For each LULC class, around 20 samples were gathered to create LULC maps.

As the LULC classification was handled by the software, it required inspecting the accuracy level of the work. The confusion matrix and kappa index were the best quantitative measurement of land cover classification accuracy and it was applied to evaluate the accuracy assessment of LULC classification (Kafy et al. 2020, 100314). Using Google Earth images 300 ground points were randomly selected for measuring the accuracy of each land cover classification. At last, the change of LULC from 2010 to 2020 was analyzed to identify the contribution of LULC to the LST and the impact of LST on the ecology of the study area.

Table 2: Description of land cover categories

Land cover type	Description
Water bodies	River, canal, reservoirs, ponds, lakes
Trees and bushes	Park, playground, trees, grassland
Agricultural land	Cropland, fallow land
Wetland vegetation	Open space, vacant land, low land
Buildup area	Residential, commercial, industrial, transportation networks.

2.4 Extraction of Land Surface Temperature (LST)

Landsat thermal bands were used to estimate the LST for the years 2010, 2015, and 2020. Thermal data in Landsat sensors were stored as digital numbers (DNs). To extract LST, DNs values of the thermal image were converted into spectral radiance reflectance and the spectral radiance images were converted to LST. The DNs of the thermal infrared band were converted into spectral radiance (L_λ) using equation (4) (Kumar, Bhaskar, and Padmakumari 2012, 771-778).

$$L_\lambda = \left\{\frac{L_{MAX} - L_{MIN}}{Q_{CALMAX} - Q_{CALMIN}}\right\} * DN - 1 * L_{MIN} \quad (4)$$

Here,

L_{MAX} = the spectral radiance that is considered to Q_{CALMAX} in W/ (m^2 * sr * μm)

L_{MIN} = the spectral radiance that is considered to Q_{CALMIN} in W/ (m^2 * sr * μm)

Q_{CALMAX} = the maximum quantized calibrated pixel value (corresponding to L_{MAX}) in DN = 255

Q_{CALMIN} = the minimum quantized calibrated pixel value (corresponding to L_{MIN}) in DN = 1.

The sensor brightness temperature (BT) also known as black body temperature was obtained from the spectral radiance using Plank's inverse function in equation (5).

$$BT = \left\{\frac{K_2}{In(1+\frac{K2}{L_\lambda})}\right\} \quad (5)$$

Here,

K_1 and K_2 are calibration constant values for a certain Landsat sensor obtained from the metadata file and BT is the brightness temperature in Kelvin.

Table 3: Calibration constant values for thermal band

Sensor	K_1 [W/ (m^2 * sr * μm)]	K_2 [W/ (m^2 * sr * μm)]
Landsat 7 ETM	666.09	1282.71

After deriving the temperature in the Kelvin unit, the LST was converted to degree celsius from equation (6)

LST (^{o}C) = BT-273.15……………………………………… (6)

ArcGIS software v10.7 was used for calculating cell statistics. After extracting LST for the years 2010, 2015, and 2020, the LST map was exported as a raster data format.

To validate the LST estimation from remotely sensed data, maximum and minimum surface temperature data for the years 16 April 2010, 20 April 2015, and 08 April 2020 in the daytime were obtained from the Bangladesh Metrological Department (BMD). The deviation was calculated between estimated LST and recorded LST. A negative deviation in LST implied that the estimated temperature was higher than the recorded temperature, while a positive deviation number indicated that the estimated temperature was lower than the recorded temperature. The deviation between estimated and recorded LST of less than 20% is acceptable and can be used for further investigations like LST simulation (Kafy et al. 2020, 11-23).

2.5 Determining urban indices (UI)

Changing LST was the consequence of changing the moisture, shrinkage of a water body, changing vegetation coverage, and other environmental parameters. Appearances or disappearances of these parameters could describe the fluctuation of LST in a certain region. These parameters might simply be correlated to UI. In the present study, some UI like NDWI, NDBI, NDVI, SAVI, and EBBI were measured to determine the ecological change for the year 2020 (Table 4). The UI was computed using digital numbers of indicated bands and reflectance of indicated bands (Mushore et al. 2017b, 397-410). As aforementioned, several indices were determined to compare the differences in the intensity of the relationship with surface temperature.

Table 4: Computation of UI for the year 2020

Index	Calculation	Reference
Normalized difference water index	$\mathrm{NDWI} = \frac{\mathrm{NIR} - \mathrm{SWIR1}}{\mathrm{NIR} + \mathrm{SWIR1}}$	(Mushore et al. 2017b, 397-410)
Normalized difference buildup index	$\mathrm{NDBI} = \frac{\mathrm{SWIR1} - \mathrm{NIR}}{\mathrm{SWIR1} + \mathrm{NIR}}$	
Normalized difference vegetation index	$\mathrm{NDVI} = \frac{\mathrm{NIR} - \mathrm{RED}}{\mathrm{NIR} + \mathrm{RED}}$	
Soil adjustment vegetation index	$\mathrm{SAVI} = \frac{\mathrm{NIR-RED}}{\mathrm{NIR+RED+L}} * (\mathrm{L} + 1)$	
Enhance bareness and buildup index	$\mathrm{EBBI} = \frac{\mathrm{SWIR1} - \mathrm{NIR}}{10\sqrt{(\mathrm{SWIR1} + \mathrm{TIRS1})}}$	

2.6 Developing a contribution index (CI)

The effect of LULC on warming or cooling in a region was determined by the type of LULC and the percentage of the total area covered by each type. Due to latent heat transfer the vegetation cover, water bodies, and trees and bushes had a surface cooling effect. Despite having a cooling impact, the overall value is determined by the proportion of the entire surface they covered. The contribution of LULC type for warming and cooling weather was calculated through the contribution index (CI) in equation (7). The CI was utilized to link spatial structure to LST intensities, as well as long-term variations in LULC. Positive values of CI indicated how much the LULC type contributes to raising the surface temperatures of the study area, while negative values indicated the contribution to alleviating surface temperature in the study area (Tarawally et al. 2018, 112).

CI=Dt * S ……………….…………………………….....……. (7)

Here, Dt denotes the difference between the average temperature of the entire study area and the average temperature of each LULC type and S is the ratio of each LULC type to the entire study area.

2.8 Identification of hot and cool areas

The hot and cool spots of the study area were identified for the year 2020 by calculating the Getis-Ord G_i^* statistic using ArcGIS for the surface temperature concerning the temperatures of nearby cells (Grigoraș and Urițescu 2018, 14-22). The calculation of the G_i^*statistics for the LST image of 2020 resulted in the assignment of a z-value to each pixel and represented where characteristics with high or low values were clustered. The Getis-Ord statistics were calculated according to equation (8) (ESRI 2018; Grigoraș and Urițescu 2018, 14-22).

$$G_i^* = \frac{\sum_{j=1}^{n} W_{i,j} Xj - \bar{X} \sum_{j=1}^{n} W_{i,j}}{S\sqrt{\frac{\left[n - \sum_{j=1}^{n} W_{i,j}^2 - \left(\sum_{j=1}^{n} W_{i,j}\right)^2\right]}{n-1}}} \quad \text{……………………….....…..(8)}$$

where i is the resultant G_i^* statistics (z-scores and p- values) for pixel i, Xj is the LST value for pixel j, $W_{i,j}$ is the spatial weight between pixel i and neighboring pixel j, n is equal to the total number of pixels, and $\bar{X}$ and S are mean and variance respectively which are calculated by equations (9) and (10).

$$\bar{X} = \frac{\sum_{j=1}^{n} Xj}{n} \quad \text{…………………………..............………..……(9)}$$

$$S = \sqrt{\frac{\sum_{j=1}^{n} Xj^2}{n} - (\bar{X})^2} \quad \text{…………………....………….……(10)}$$

The output of the G_i^*statistic (the z-score) denoted the statistical significance of clustering for a given distance whereas the p-value represented the likelihood (ESRI 2018). To define the 'Hot and Cold' spots, the suitable threshold for the z-value was determined. The z value was compared to the range of values in Table 5 for seven different confidence levels. Usually, a z-value over 2.58 (99% confidence level) indicated a statistically significant result (Mavrakou et al. 2018, 16).

Table 5: Classification of Khulna area based on p and z values

Significance level (p-Value)	Critical value (z Score)	Confidence level	Classified area
-0.01	<-2.58	99%	Very cold spot
-0.05	-2.58 - -1.96	95%	Cold spot
-0.10	-1.96 - -1.65	90%	Cool spot
0	-1.65 - 1.65	-	Not significant
0.10	1.65 – 1.96	90%	Warm spot
0.05	1.96 – 2.58	95%	Hot spot
0.01	>2.58	99%	Very hot spot

3. Results and discussion

3.1 LULC scenario in the study area

After performing MLSC in the Landsat data, the changes in the LULC pattern were detected for the past 10 years (2010-2020) (Fig. 2). Two trends of land cover changes were visible; firstly, the buildup area was gradually increased and secondly, the water bodies, trees and bushes, agricultural land, and wetland vegetation declined during the study period. Several circumstances have contributed to the increase in the urban area and bare land. The water bodies, trees and bushes, agricultural land, and wetland vegetation were rapidly transformed into buildup areas to meet the demand of the vast population for residential, commercial, and institutional purposes.

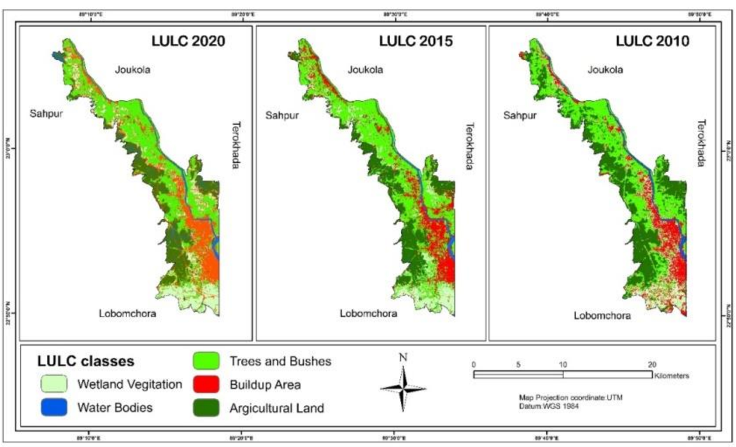

Figure 2: LULC change of the study area for the years 2020, 2015, and 2010

The total LULC change of the entire area from 2010-2020 was revealed in Table 6 and Fig. 3 which represented the net changes of overall LULC classes from the years 2010 to 2020. The water bodies in the study area were 7.79 sqr km in 2010 but it was turned into 5.91 sqr km and 4.88 sqr km in the year 2015 and 2020 respectively. The overall water bodies decreased by 37.34% from 2010-2020. Trees and Bushes were 72.84 sqr km in 2010 and after five and ten years they reached 69.41 sqr km and 71.53 sqr km. The loss of trees and bushes coverage was 1.80% from 2010 to 2020. In 2010, the agricultural land was 45.83 sqr km of the entire area which reached 47.39 sqr km in 2015. But the area of agricultural land was reduced to 42.95 sqr km in 2020. Around 6.28% of agricultural land was reduced in the study region of 2010-2020. The wetland vegetation was 34.34 sqr km in 2010, which decreased to 30.12 sqr km in 2015. In 2020, it occupied 30.63 sqr km resulting in the overall wetland vegetation being reduced by 10.81% during the study period. The buildup area was 44.37 sqr km in 2010, and the buildup area in the study region was expanded to 49.55 sqr km and 52.45 sqr km in 2015 and 2020 year respectively. The growth of the buildup area increased by 18.20% from 2010-2020. Especially the buildup area was increased in the Khulna coastal urban area from time to time. As there was the second-largest seaport and different types of industries were situated in the study area, the LULC was changed continuously.

Table 6: LULC scenario of the study area from 2010 to 2020

LULC Type	Area (sqr km)		
	2010	2015	2020
Water bodies	7.79	5.91	4.88
Trees and bushes	72.84	69.41	71.53
Agricultural land	45.83	47.39	42.95
Wetland vegetation	34.34	30.12	30.63
Buildup area	44.37	49.55	52.45

Table 7 demonstrated the classification accuracy and Kappa coefficient of land use classification. The classification accuracy for each period was over 88% and in 2020, the classification accuracy was higher compared to 2010 and 2015. The value of the Kappa coefficient was more than 0.85 for all images. When the value of the Kappa coefficient was above 0.75, it implied that the degree of accuracy was categorized as very good. A comparison was made between the sampling points (300 points) and their corresponding point on Google Earth images from the same period to validate the LULC classifications. For all periods, the validation results are more than 87%. So, overall accuracy assessments, Kappa coefficient statistics, and validation all indicated that the accuracy was good.

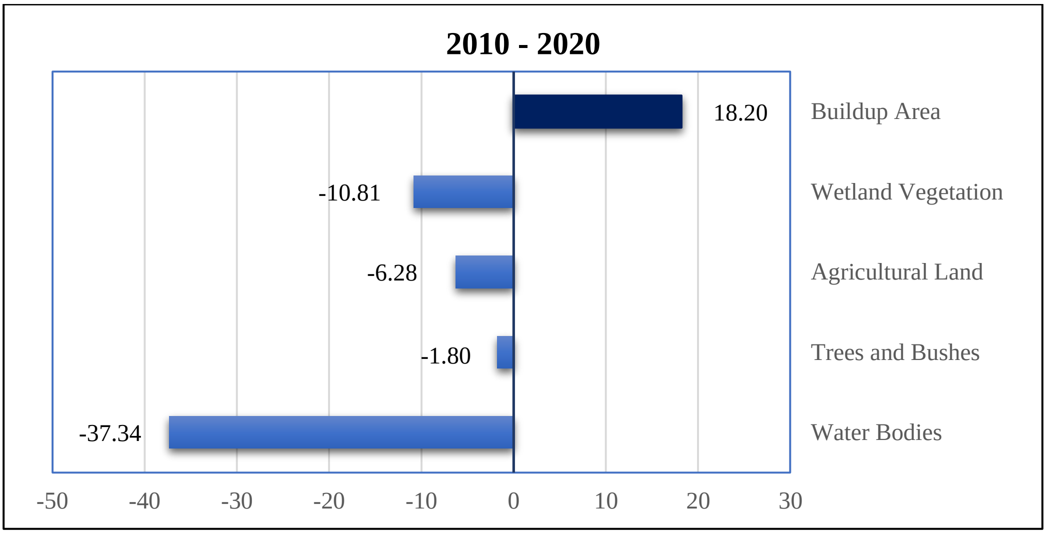

Figure 3: Net changes of LULC classes in percentage from 2010 to 2020

Table 7: Accuracy assessment of LULC

Accuracy	2010	2015	2020
Classification accuracy (%)	88.76	90.68	91.47
Kappa coefficient	0.85	0.86	0.87
Validation (%)	89.86	87.91	90.76

3.2 Land surface temperature (LST) mapping

The variation of LST distribution in three phases e.g. 2010, 2015, and 2020 were presented in Fig. 4. The dark reddish color showed high temperatures and the pale reddish color showed low temperatures on all maps. Maximum LST was found at 29.97 ^{o}C in 2010 and it was increased up to 32 ^{o}C and 36.91 ^{o}C in the years 2015 and 2020 respectively. It seemed that the LST of the study region was rising dramatically. From 2010 to 2020, around 6.94 ^{o}C maximum and 3.54 ^{o}C minimum surface temperatures increased in Khulna. The reasons for these might be the decrease of water bodies and the increase in buildup area. It was also found that the area near the Central Business District (CBD) was highly affected by the high level of surface temperature while the peripheral areas were less affected.

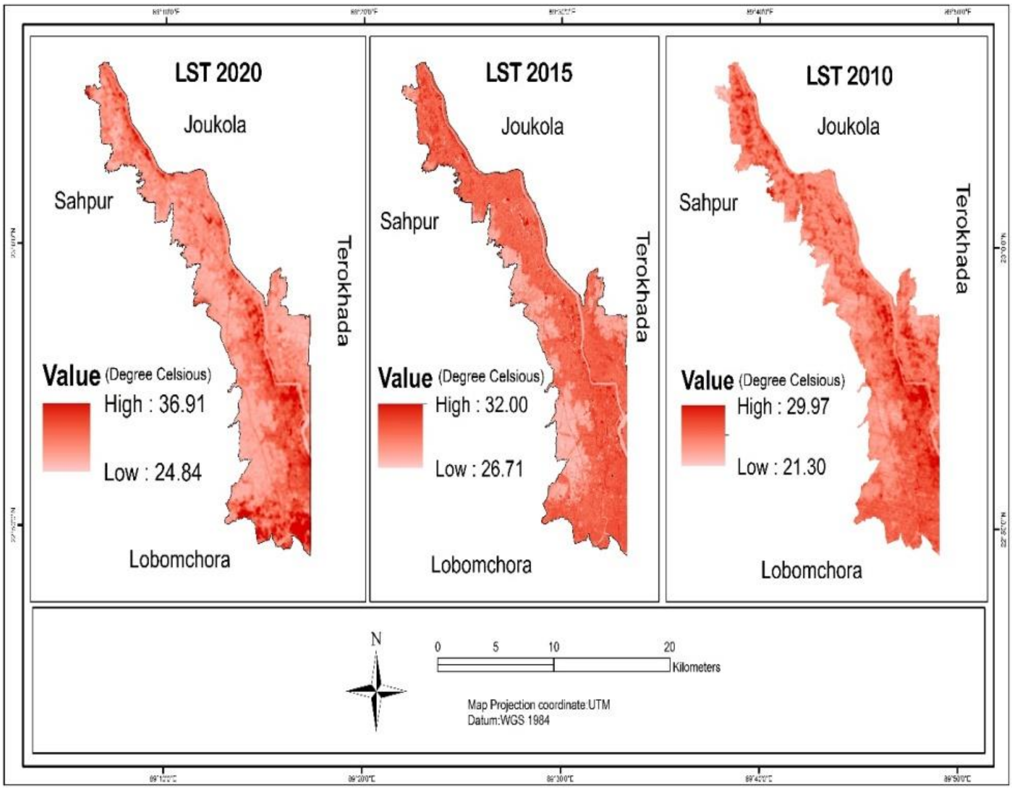

Figure 4: LST scenario of the study area for the years 2010, 2015, and 2020

To validate the LST estimation from remotely sensed data maximum and minimum surface temperature data were obtained from the BMD for April 2010, 2015, and 2020 in the daytime. The deviations were estimated using BMD's LST estimation data (Table 8). A negative deviation in LST indicated that the estimated temperature was greater than the recorded temperature, while a positive deviation value indicated that the estimated temperature was lower than the recorded temperature. According to BMD estimation, the highest variation was found in the minimum temperature for the year 2010 (13.41 %), and the lowest deviation was found in the maximum temperature for the year 2020 (-4.56%). In the last ten years, the temperature difference between remotely sensed estimated and BMD recorded LST was 6.94 ^{o}C and 3.3 ^{o}C, respectively. The difference between estimated and recorded LST was less than 20% in this case.

Table 8: Validation of LST from remotely sensed data

Year / Source of estimated/ recorded LST	2010		2015		2020	
	Maximum	Minimum	Maximum	Minimum	Maximum	Minimum
Remotely sensed estimated LST (ºC)	29.97	21.3	32	26.71	36.91	24.84
BMD recorded LST (ºC)	32	24.6	34.9	24.1	35.3	23.7
Deviation (ºC)	2.03	3.3	2.9	-2.61	-1.61	-1.14
Deviation (%)	6.34	13.41	8.31	-10.83	-4.56	-4.81

3.3 LULC responses to LST

The LST distribution of LULC categories across the study region for 2010, 2015, and 2020 was shown in Fig. 5. This analysis indicated that the average surface temperature of water bodies, trees and bushes, agricultural land, and wetland vegetation was comparatively lower than the buildup area. This pattern was caused by the greater heat absorption capacity of the buildup area than the natural surroundings which similarly contributes to higher temperatures in towns and cities.

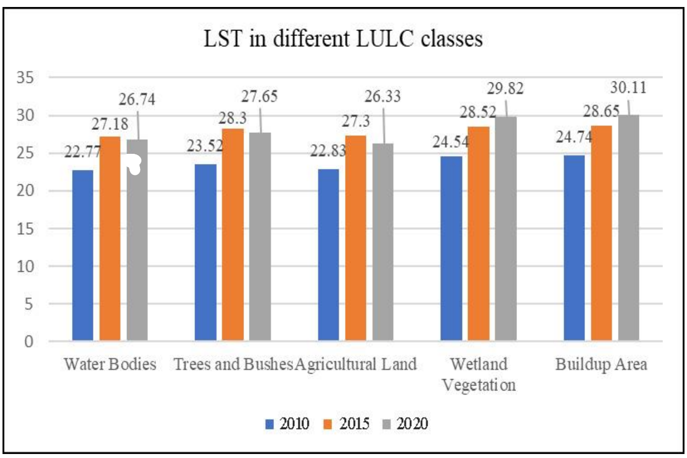

Figure 5: LST (mean) in different LULC Categories from 2010 to 2020

As water bodies, trees and bushes, wetland vegetation, and agricultural land had a propensity to latent heat transfer, it might help to mitigate the surface temperature. On the other hand, the buildup area had an extreme heat absorption capacity which had a detrimental impact on the surface temperature. The negative value of CI mentioned that it was competent to mitigate LST in the study area while the positive value of CI expounded that it was responsible to increase LST (Table 9). The results of the CI represented that the water bodies (-0.019) and agricultural land (-0.153) had a significant cooling effect in the study area which mitigated the surface temperature. The cooling effect of agricultural land was more than that of water bodies in the study area. The wetland vegetation had a warming effect and their contribution remained minimal over the study area. Besides, the trees and bushes had a more warming effect in the region as indicated by the CI of 0.107. But the buildup area contributed more to increasing the LST in the entire study area. The warming effect of the buildup area was high as indicated by the CI of 0.168. The buildup area was increased in the study region as a consequence of urbanization and it accelerated the promotion of LST as CI described. Depending on the LULC change it was found that an 18.20% increase in buildup area increased 5.37 ^{o}C LST from 2010 to 2020 (Fig. 3 & Fig. 5).

Table 9: Computation of CI to know LULC contribution in LST

LULC type	Dt	S	CI
Water bodies	-0.81	0.02	-0.02
Trees and bushes	0.31	0.35	0.11
Agriculture land	-0.69	0.22	-0.15
Wetland vegetation	0.53	0.15	0.08
Buildup area	0.66	0.26	0.17

3.4 Calculating urban indices (UI)

Fig. 6 represents the aftermath of UI like NDWI, NDBI, NDVI, SAVI, and EBBI. Here, the high value of vegetation and water index were 0.58 and 0.54 respectively which mentioned that the area of vegetation and water bodies were less in a proportion of the total entire study area. As a result, the surface temperature was increased in Khulna. At the same time, the high value of NDBI and EBBI mentioned that the bare land and buildup area were increased in Khulna dramatically which had a great contribution to raising the surface temperature. The reason behind that the vegetation cover and water bodies were transformed into buildup areas and bare land to meet the demand of the vast population in Khulna. Every year the population increased and for that, unplanned development occurred in Khulna. Due to this unplanned urbanization, the vegetation cover and water bodies decreased in 2020 which increased the surface temperature.

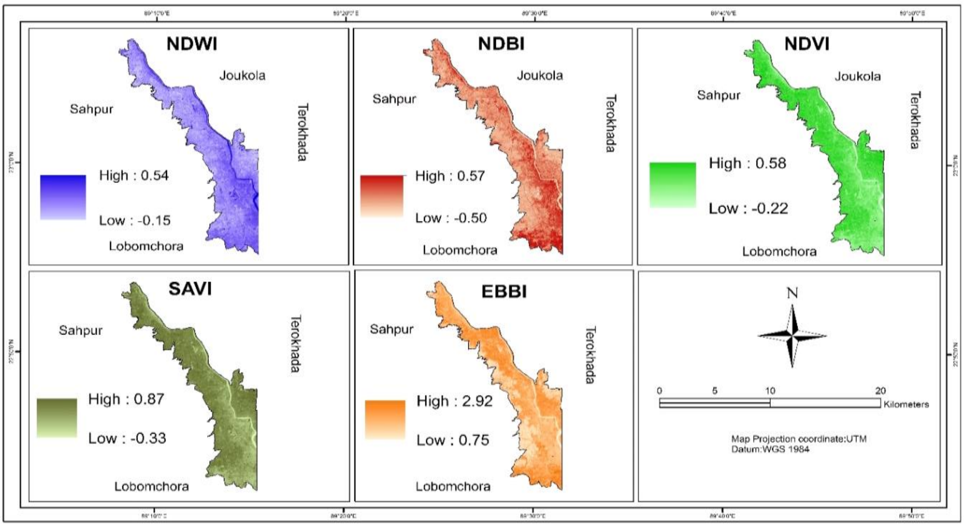

Figure 6: Computation of UI map for the year 2020

3.5 Hot and cool location in the study area for 2020

The hot and cold spots of the study area were identified for the year 2020 by using the Getis-Ord G_i^* statistic where a higher z value indicated the hot location and a lower z value indicated the cold location (Fig. 7). In order to define the “hot spot” areas, the suitable threshold for the z-values was determined as follows in Table 5. The z-values over 2.58 were recognized as hot locations and z-values less than -2.58 were defined as cold locations. The Mouzas with a greater LST value were depicted as ‘hot spots, while those with lower LST values, were labeled as ‘cold spots’.

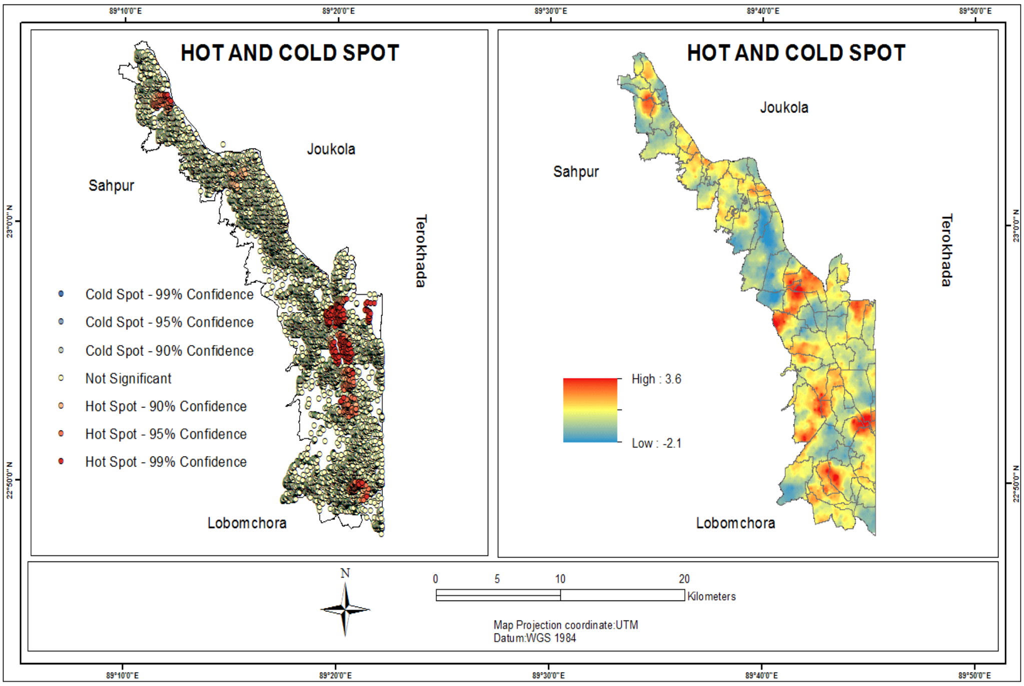

Figure 7: Hot and cool spots analysis map of the study area for 2020

Table 10 represents the hot locations where about 28 Mouzas (about 93.73 sqr km of the total area) fell in hot islands and 53 Mouzas (108.81 sqr km of the total area) were characterized as cold islands according to the analysis. The hot spots were generated as a result of substantially increasing buildup area and bare land with a homogenous land cover of impervious materials, as well as decreasing vegetation and water bodies.

Table 10: Hot places (Mouza name) in the study area for 2020

Serial no	Mouza name	Serial no	Mouza name
1	Brahmaganti	15	Krishnonagar
2	Maheshwarpur	16	Lakshmipur
3	Paginate	17	Maheswarpasha
4	Aaronghata	18	Mohakal
5	BilPabla	19	Pabla
6	Boyra	20	Paygram
7	ChotoBoyra	21	Rajghat
8	DakshinDihi	22	Rayermahal
9	Deyana	23	Shanchibunia
10	Dhopadi	24	Shiromoni
1	Durgapur	25	Taliganti
12	Ektarpur	26	Taribpur
13	Gilatala	27	Thikrabandh
14	Goalpara	28	Maheswarpasha

4. Conclusion & Recommendation

- LST is a crucial parameter of the urban environment. Imbalanced LST can bring an ecological threat to all animals including human lives. This study has been designed for assessing the changes in LULC and LST from 2010 to 2020 in the coastal urban region (KDA Khulna). The aftermath has demonstrated that it has been identified the hot and cool locations in the research area. The results have represented that almost 19 % of buildup area increased in 2020 and it dominates the loss of wetland vegetation (-10.81%), water bodies (-37.34%), agricultural land (-6.28%), and trees and bushes (-1.80%). It has been also mentioned that maximum and minimum LST have increased by about 7 ^{o}C and 3.50 ^{o}C in the past 10 years.
- The LST distribution in different LULC categories represents that the highest temperature has been recorded in the buildup area and it has a warming effect on the Khulna territory. On the other hand, water bodies, trees and bushes, wetland vegetation, and agricultural land have experienced the lowest temperature and among these LULC types, the water bodies and agricultural land have a significant cooling effect on the Khulna region which mitigate the surface temperature.

Besides, the wetland vegetation had a minimal warming effect on the area. About 28 Mouzas were considered hot islands and 53 Mouzas were identified as cold islands in the study area. If such circumstances will be continued, the amount of 'hot spots' will be increased in the next decade which will result in an ecological threat to human beings.

- Since Khulna is one of the coastal areas out of 19 coastal areas in Bangladesh and due to the location of Sundarbans, the region has a significant impact on the environment. So, it's high time for the relevant authorities to pay attention to ecological change issues in Khulna otherwise the quality of life will continue to be jeopardized. This study will be helpful for government officials, policymakers politicians, and urban planners of Khulna City, who can depict the hot and cold spots, and also utilize the funding of this study for future planning and decision-making.

References

Ahmed, Bayes. 2011. "Modelling spatio-temporal urban land cover growth dynamics using remote sensing and GIS techniques: A case study of Khulna City." *J. Bangladesh Instit. Plan* 4 (1633):43.

Ahmed, Bayes, Md Kamruzzaman, Xuan Zhu, Md Rahman, and Keechoo Choi. 2013. "Simulating land cover changes and their impacts on land surface temperature in Dhaka, Bangladesh." *Remote Sensing* 5 (11):5969-5998.

Balew, Abel, and Tesfaye Korme. 2020. "Monitoring land surface temperature in Bahir Dar city and its surrounding using Landsat images." *The Egyptian Journal of Remote Sensing and Space Science*.

Balogun, IA, and KA Ishola. 2017. "Projection of future changes in landuse/landcover using cellular automata/markov model over Akure city, Nigeria." *Journal of Remote Sensing Technology* 5 (1):22-31.

BBS. 2019. Statistical year book 2018. In *Bangladesh Bureau of Statistics; Ministry of Planning; Government of The People's Republic of Bangladesh*.

Chapa, Fernando, Srividya Hariharan, and Jochen Hack. 2019. "A New Approach to High-Resolution Urban Land Use Classification Using Open Access Software and True Color Satellite Images." *Sustainability* 11 (19):5266.

Chen, Xiao-Ling, Hong-Mei Zhao, Ping-Xiang Li, and Zhi-Yong Yin. 2006. "Remote sensing image-based analysis of the relationship between urban heat island and land use/cover changes." *Remote sensing of environment* 104 (2):133-146.

Chun, Bumseok, and J-M Guldmann. 2014. "Spatial statistical analysis and simulation of the urban heat island in high-density central cities." *Landscape and urban planning* 125:76-88.

Dasgupta, Susmita, Farhana Akhter Kamal, Zahirul Huque Khan, Sharifuzzaman Choudhury, and Ainun Nishat. 2015. "River salinity and climate change: evidence from coastal Bangladesh." In *world scientific reference on asia and the world economy*, 205-242. World Scientific.

El-Zeiny, Ahmed M, and Hala A Effat. 2017. "Environmental monitoring of spatiotemporal change in land use/land cover and its impact on land surface temperature in El-Fayoum governorate, Egypt." *Remote sensing applications: society and environment* 8:266-277.

Elagouz, MH, SM Abou-Shleel, AA Belal, and MAO El-Mohandes. 2019. "Detection of land use/cover change in Egyptian Nile Delta using remote sensing." *The Egyptian Journal of Remote Sensing and Space Science*.

Esraz-Ul-Zannat, Md. 2012. "Study on land use policies of khulna structure plan 2000-2020 in the light of climate change induced flood scenario."

ESRI. 2018. How Hot Spot Analysis: Getis-Ord Gi* (Spatial Statistics) works

Fu, Peng, and Qihao Weng. 2018. "Responses of urban heat island in Atlanta to different land-use scenarios." *Theoretical and Applied Climatology* 133 (1-2):123-135.

Gao, Bo-Cai. 1995. "Normalized difference water index for remote sensing of vegetation liquid water from space." Imaging Spectrometry.

Grigoraș, Georgiana, and Bogdan Urițescu. 2018. "Spatial Hotspot Analysis of Bucharest's Urban Heat Island (UHI) Using Modis Data." *Annals of Valahia University of Targoviste, Geographical Series* 18 (1):14-22.

Guo, Guanhua, Zhifeng Wu, Rongbo Xiao, Yingbiao Chen, Xiaonan Liu, and Xiaoshi Zhang. 2015. "Impacts of urban biophysical composition on land surface temperature in urban heat island clusters." *Landscape and Urban Planning* 135:1-10.

Halmy, Marwa Waseem A, Paul E Gessler, Jeffrey A Hicke, and Boshra B Salem. 2015. "Land use/land cover change detection and prediction in the north-western coastal desert of Egypt using Markov-CA." *Applied Geography* 63:101-112.

Jain, Shweta, Srikanta Sannigrahi, Somnath Sen, Sandeep Bhatt, Suman Chakraborti, and Shahid Rahmat. 2020. "Urban heat island intensity and its mitigation strategies in the fast-growing urban area." *Journal of Urban Management* 9 (1):54-66.

Kafy, Abdulla-Al, Mohammad Mahmudul Hasan, Muhaiminul Islam, and Md Shahinoor Rahman. 2020. "Modelling future land use land cover changes and their impacts on land surface temperatures in Rajshahi, Bangladesh." *Remote Sensing Applications: Society and Environment*:100314.

Kafy, Abdulla Al, Abdullah-Al Faisal, Soumik Sikdar, Mohammad Hasan, Mahbubur Rahman, Mohammad Hasib Khan, and Rahatul %J Journal of Geographical Studies Islam. 2020. "Impact of LULC changes on LST in Rajshahi district of Bangladesh: a remote sensing approach." 3:11-23.

Kumar, K Sundara, P Udaya Bhaskar, and K Padmakumari. 2012. "Estimation of land surface temperature to study urban heat island effect using LANDSAT ETM+ image." *International journal of Engineering Science technology* 4 (2):771-778.

Li, Long, Yong Zha, and Jiahua Zhang. 2020. "Spatially non-stationary effect of underlying driving factors on surface urban heat islands in global major cities." *International Journal of Applied Earth Observation and Geoinformation* 90:102131.

Lilly Rose, A, and Monsingh D Devadas. 2009. "analysis of land surface temperature and land use/land cover types using remote sensing imagery-a case in chennai city, india." The seventh international conference on urban clim held on.

Maimaitiyiming, Matthew, Abduwasit Ghulam, Tashpolat Tiyip, Filiberto Pla, Pedro Latorre-Carmona, Ümüt Halik, Mamat Sawut, and Mario Caetano. 2014. "Effects of green space spatial pattern on land surface temperature: Implications for sustainable urban planning and climate change adaptation." *ISPRS Journal of Photogrammetry and Remote Sensing* 89:59-66.

Mavrakou, Thaleia, Anastasios Polydoros, Constantinos Cartalis, and Mat Santamouris. 2018. "Recognition of thermal hot and cold spots in urban areas in support of mitigation plans to counteract overheating: Application for Athens." *Climate* 6 (1):16.

Mishra, Varun Narayan, and Praveen Kumar Rai. 2016. "A remote sensing aided multi-layer perceptron-Markov chain analysis for land use and land cover change prediction in Patna district (Bihar), India." *Arabian Journal of Geosciences* 9 (4):249.

Mushore, Terence Darlington, John Odindi, Timothy Dube, and Onisimo Mutanga. 2017a. "Prediction of future urban surface temperatures using medium resolution satellite data in Harare metropolitan city, Zimbabwe." *J Building Environment* 122:397-410.

Mushore, Terence Darlington, John Odindi, Timothy Dube, and Onisimo Mutanga. 2017b. "Prediction of future urban surface temperatures using medium resolution satellite data in Harare metropolitan city, Zimbabwe." *Building and Environment* 122:397-410.

Mustafa, Elhadi K, Yungang Co, Guoxiang Liu, Mosbeh R Kaloop, Ashraf A Beshr, Fawzi Zarzoura, and Mohammed Sadek. 2020. "Study for Predicting Land Surface Temperature (LST) Using Landsat Data: A Comparison of Four Algorithms." *Advances in Civil Engineering* 2020.

Pal, Swades, and SK Ziaul. 2017. "Detection of land use and land cover change and land surface temperature in English Bazar urban centre." *The Egyptian Journal of Remote Sensing and Space Science* 20 (1):125-145.

Perugini, Lucia, Luca Caporaso, Sergio Marconi, Alessandro Cescatti, Benjamin Quesada, Nathalie de Noblet-Ducoudre, Johanna I House, and Almut Arneth. 2017. "Biophysical effects on temperature and precipitation due to land cover change." *Environmental Research Letters* 12 (5):053002.

Rahman, Muhammad Tauhidur, Adel S Aldosary, and Md Mortoja. 2017. "Modeling future land cover changes and their effects on the land surface temperatures in the Saudi Arabian eastern coastal city of Dammam." *Land* 6 (2):36.

Rasul, Azad. 2020. "Global Spatial Relationship between Land Use Land Cover and Land Surface Temperature."

Ren, Hongrui, Guangsheng Zhou, and Feng Zhang. 2018. "Using negative soil adjustment factor in soil-adjusted vegetation index (SAVI) for aboveground living biomass estimation in arid grasslands." *Remote Sensing of Environment* 209:439-445.

Solanky, Vijay, Sangeeta Singh, and SK Katiyar. 2018. "Land Surface Temperature Estimation Using Remote Sensing Data." In *Hydrologic Modeling*, 343-351. Springer.

Tan, Kok Chooi, HS Lim, MZ MatJafri, and Khiruddin Abdullah. 2009. "Study on Land Surface Temperature Based on Landsat Image over Penang Island, Malaysia." 2009 Sixth International Conference on Computer Graphics, Imaging and Visualization.

Tarawally, Musa, Wenbo Xu, Weiming Hou, and Terence Darlington Mushore. 2018. "Comparative analysis of responses of land surface temperature to long-term land use/cover changes between a coastal and Inland City: A case of Freetown and Bo Town in Sierra Leone." *Remote Sensing* 10 (1):112.

Tran, Duy X, Filiberto Pla, Pedro Latorre-Carmona, Soe W Myint, Mario Caetano, and Hoan V Kieu. 2017. "Characterizing the relationship between land use land cover change and land surface temperature." *ISPRS Journal of Photogrammetry and Remote Sensing* 124:119-132.

Trolle, Dennis, Anders Nielsen, Hans E Andersen, Hans Thodsen, Jørgen E Olesen, Christen D Børgesen, Jens Chr Refsgaard, Torben O Sonnenborg, Ida B Karlsson, and Jesper P Christensen. 2019. "Effects of changes in land use and climate on aquatic ecosystems: Coupling of models and decomposition of uncertainties." *Science of the Total Environment* 657:627-633.

Voogt, James A, and Tim R Oke. 2003. "Thermal remote sensing of urban climates." *Remote sensing of environment* 86 (3):370-384.

Wu, Jianguo, G Darrel Jenerette, Alexander Buyantuyev, and Charles L Redman. 2011. "Quantifying spatiotemporal patterns of urbanization: The case of the two fastest growing metropolitan regions in the United States." *Ecological Complexity* 8 (1):1-8.

Zha, Yong, Jay Gao, and Shaoxiang Ni. 2003. "Use of normalized difference built-up index in automatically mapping urban areas from TM imagery." *International journal of remote sensing* 24 (3):583-594.